Published in final edited form as:
Acta Biomater. 2013 July ; 9(7): 7399–7409. doi:10.1016/j.actbio.2013.03.027.

Acoustic droplet–hydrogel composites for spatial and temporal control of growth factor delivery and scaffold stiffness

Mario L. Fabiilli[a,*,1], **Christopher G. Wilson**[b,1], **Frédéric Padilla**[a,c], **Francisco M. Martín-Saavedra**[d], **J. Brian Fowlkes**[a,e], and **Renny T. Franceschi**[b,e]

[a]Department of Radiology, University of Michigan Health System, Ann Arbor, MI, USA

[b]Center for Craniofacial Regeneration, University of Michigan School of Dentistry, Ann Arbor, MI, USA

[c]Institut National de la Santé et de la Recherche Médicale (INSERM) U556, Lyon, France

[d]Hospital Universitario La Paz-IdiPAZ & CIBER-BBN, Madrid, Spain

[e]Department of Biomedical Engineering, University of Michigan, Ann Arbor, MI, USA

Abstract

Wound healing is regulated by temporally and spatially restricted patterns of growth factor signaling, but there are few delivery vehicles capable of the “on-demand” release necessary for recapitulating these patterns. Recently we described a perfluorocarbon double emulsion that selectively releases a protein payload upon exposure to ultrasound through a process known as acoustic droplet vaporization (ADV). In this study, we describe a delivery system composed of fibrin hydrogels doped with growth factor-loaded double emulsion for applications in tissue regeneration. Release of immunoreactive basic fibroblast growth factor (bFGF) from the composites increased up to 5-fold following ADV and delayed release was achieved by delaying exposure to ultrasound. Releasates of ultrasound-treated materials significantly increased the proliferation of endothelial cells compared to sham controls, indicating that the released bFGF was bioactive. ADV also triggered changes in the ultrastructure and mechanical properties of the fibrin as bubble formation and consolidation of the fibrin in ultrasound-treated composites were accompanied by up to a 22-fold increase in shear stiffness. ADV did not reduce the viability of cells suspended in composite scaffolds. These results demonstrate that an acoustic droplet–hydrogel composite could have broad utility in promoting wound healing through on-demand control of growth factor release and/or scaffold architecture.

Keywords

Acoustic droplet vaporization; Controlled drug release; Fibrin; Fibroblast growth factor; Fluorocarbon

*Corresponding author. Tel.: +1 734 647 9326; fax: +1 734 764 8541. mfabiill@umich.edu. .

[1]These authors contributed equally to this work.

Appendix A. Figures with essential colour discrimination Certain figures in this article, particularly Figs. 1, 3, 5 and 7 are difficult to interpret in black and white. The full colour images can be found in the on-line version, at http://dx.doi.org/10.1016/j.actbio.2013.03.027.

Appendix B. Supplementary data Supplementary data associated with this article can be found, in the online version, at http://dx.doi.org/10.1016/j.actbio.2013.03.027.

1. Introduction

Scaffolds, typically fabricated with porous structures and composed of biodegradable materials, are frequently used in regenerative medicine as an adhesive substrate for the attachment of cells and/or the encapsulation of inductive proteins (e.g. growth factors) [1–3]. As a critical component of the local, cellular microenvironment, growth factors can affect the migration, survival, proliferation and differentiation of cells. In most cases, the release of growth factors, either chemically conjugated to the scaffold material [4,5] or physically contained within particulates [6–8], is a process dominated by molecular diffusion and material degradation. The ability to modulate growth factor release from these passive systems is severely limited, especially after in vivo implantation of the scaffold.

Non-invasive control of protein release from a scaffold could improve the efficacy and safety of growth factor-based therapies. Additionally, such control could facilitate the generation of distinct spatial and/or temporal profiles of growth factor availability within the scaffold, thus more closely mimicking the patterns of growth factor expression observed during endogenous wound healing [9,10]. Various stimuli such as pH [11] and proteases [12], as well as energy-based stimuli such as magnetism [13,14], electricity [15], light [16], and temperature [17], have been used to trigger the release of therapeutic agents. However, the ability to translate these externally modulated systems to the clinic is limited by the inability to focus the triggering stimulus or interact with deep tissue implants.

In addition to responding to chemical signals such as growth factors, cells also respond to the mechanical properties of their microenvironment [18]. Within a scaffold, physical properties such as elasticity, pore size, and degradation rate affect cellular processes [19,20], and on-demand perturbation of those properties would provide new avenues by which to “actively” regulate cell behavior in an engineered tissue. Although a recent study demonstrated the externally controlled modification of ferrogel architecture post-implantation [14], most modifications to scaffold architecture are done prior to cell seeding and scaffold implantation [21,22] due to the use of chemicals or processing techniques that are not biocompatible [2].

One externally applied stimulus capable of inducing “on-demand” release of growth factors and scaffold architecture modification is ultrasound. Using both thermal and non-thermal mechanisms, ultrasound has been used extensively to facilitate the regeneration of both soft tissue and bone [23–25]. Ultrasound is an attractive stimulus for interacting with scaffolds since it can be applied non-invasively, focused with sub-millimeter precision, and delivered in a spatio-temporally controlled manner to sites deep within the body. The ultrasound-based mechanism used in the presented studies is termed acoustic droplet vaporization (ADV), whereby an emulsion (i.e. surfactant-stabilized, liquid droplets) is converted into gas bubbles upon exposure to ultrasound beyond a threshold pressure amplitude [26,27]. ADV has been studied as a release mechanism for therapeutic agents, primarily with emulsions designed to be delivered intravascularly [28–35]. Acoustically sensitive emulsions that undergo ADV are composed of a perfluorocarbon (PFC) liquid such as perfluoropentane (PFP, C_5F_{12}, 29 °C boiling point). At normal body temperature (i.e. 37 °C), micron-sized PFP emulsions do not vaporize due to the increase in internal (i.e. Laplace) pressure, and hence boiling point elevation, of PFP when formulated as droplets [36,37]. During ADV, the PFC liquid is converted into a gas in a microsecond timeframe [38] via a non-thermal mechanism [39]. PFCs, which have been used in medical applications as blood substitutes [40] and ultrasound contrast agents [41], are inert and biocompatible, with exhalation being the main route of excretion for low molecular weight PFCs, such as PFP, that are intravascularly administered [42]. Due to their extreme hydrophobicity and lipophobicity [43], PFCs are poor solvents for therapeutic agents such as growth factors. Therefore, for

water-soluble agents such as growth factors, a double emulsion of the form water-in-PFC-in-water (W_1/PFC/W_2) is used to contain growth factor within the W_1 phase [32,34,44,45]. The PFC within the double emulsion serves multiple functions. First, the PFC – which is exceedingly hydrophobic [43] – acts as a diffusion barrier for the hydrophilic payload contained within the W_1 phase droplets. Second, during ADV, the PFC undergoes a liquid-to-gas phase transition, thus dispersing the W_1 phase droplets and facilitating release of the encapsulated growth factor.

In the presented in vitro studies, droplet–hydrogel composites – consisting of a fibrin matrix doped with a PFC double emulsion – were generated. These novel composites provide a uniquely bioactive platform that enables the noninvasive regulation, both spatially and temporally, of biochemical and mechanical stimuli relevant to tissue regeneration. Fibrin was chosen for the hydrogel because it has been used extensively in tissue engineering studies, polymerizes rapidly under mild conditions, and is approved by the US Food and Drug Administration (FDA) for clinical use. The experiments focus on characterizing several formulations of the composites before and after ADV in terms of (1) morphological and mechanical properties, (2) the release of bioactive, basic fibroblast growth factor (bFGF) contained within the W_1 phase, (3) enzymatic and cell-based fibrinolysis of the scaffold and (4) viability of cells co-encapsulated in the composite scaffold. These composites may be useful in tissue regeneration where bFGF has been shown to induce angiogenic [46,47] or osteogenic [48,49] responses.

2. Materials and methods

2.1. Emulsion preparation and characterization

The double emulsion was prepared by modifying a previously published method [32]. The primary emulsion (W_1/PFC) was formed by dissolving Krytox 157 FSL (CAS# 51798-33-5, DuPont, Wilmington, DE, USA), a perfluoroether with carboxylic acid functionality and Krytox 157 FSL-polyethylene glycol copolymer in PFP (CAS# 678-26-2, Strem Chemicals, Inc., Newburyport, MA, USA) at concentrations of 0.5% (w/w) and 1.0% (w/w), respectively. Krytox, including its derivatives and copolymers, has been used to stabilize emulsions in in vitro studies with mammalian cells and *Caenorhabditis elegans* [50] as well as in in vivo studies with chicken embryos [45] and rats [34]. The PFP phase was then combined with an aqueous solution of bFGF, reconstituted at 50 $\mu g\ ml^{-1}$ in phosphate buffered saline (PBS) containing 1% (w/v) bovine serum albumin (BSA) and 10 $\mu g\ ml^{-1}$ heparin, at a volumetric ratio of 2.1:1. Heparin was included because it has been shown to protect bFGF from degradation [51]. The phases were emulsified, while in an ice bath, using the microtip accessory of a sonicator (model 450, 20 kHz, Branson, Danbury, CT, USA) operating at 125 W cm^{-2} for 30 s in continuous mode. The resulting primary emulsion was added drop-wise at a 1:2 volumetric ratio to a 10 mg ml^{-1} solution of Poloxamer 188 (Sigma–Aldrich, St Louis, MO, USA), dissolved in PBS containing 1% (w/v) BSA and 10 $\mu g\ ml^{-1}$ heparin, which was in an ice bath and being stirred at 1100 rpm for 10 min. To minimize carryover of non-emulsified bFGF, the double emulsion was washed by allowing the emulsion to settle, removing the supernatant, and adding fresh PBS with 1% BSA and 10 $\mu g\ ml^{-1}$ heparin. The concentration of bFGF in the supernatant was assessed using an enzyme-linked immunosorbent assay (ELISA) (DY233, R&D Systems, Inc., Minneapolis, MN, USA). The emulsion was sized using a Coulter counter (Multisizer 3, Beckman Coulter Inc., Brea, CA, USA). Except for the bFGF release experiments, sham double emulsions were used, which did not contain bFGF in the W_1 phase. To assess the double emulsion structure, fluorescein sodium salt (Sigma–Aldrich) was dissolved in the W_1 phase. The resulting emulsion was diluted in PBS and mounted on a microscope slide in a coverwell imaging chamber (Electron Microscopy Sciences, Hatfield, PA). Confocal fluorescent images of the droplets were taken using an inverted SP5X microscope with a 63× objective

(Leica, Wetzlar, Germany). For all experiments, the emulsion was used "as is" without any further purification or size separation.

2.2. Hydrogel fabrication

Fibrin gels and droplet–hydrogel composites with either 5 or 10 mg ml^{-1} clottable protein were prepared by combining bovine fibrinogen (Sigma–Aldrich) dissolved in Dulbecco's modified Eagle medium (DMEM), with bovine thrombin (2 U ml^{-1}, Thrombin-JMI, King Pharmaceuticals, Bristol, TN, USA), and 0%, 1% or 5% (v/v) of the double emulsion. All solutions besides the emulsion were degassed under vacuum prior to polymerization. Gels were allowed to polymerize for 30 min at room temperature prior to use. For cell culture and bFGF release studies, 0.5 ml gels (final dimensions: 16 mm diameter, 2 mm height) were cast in wells of 24-well culture plates (Fisher Scientific, Pittsburgh, PA, USA). For mechanical testing, 2.5 ml gels (final dimensions: 36 mm diameter, 2 mm height) were cast in six-well HT Bioflex plates (Flexcell International Co., Hillsborough, NC, USA). In some experiments the gels were doped with Alexa Fluor 647 (AF647)-fibrinogen (Invitrogen, Grand Island, NY, USA). A summary of the composite hydrogel formulations can be seen in Table 1.

2.3. Ultrasound exposure

A calibrated 3.5 MHz single-element transducer (1.9 cm diameter, 3.81 cm focal length, A381S, Panametrics, Olympus NDT, Waltham, MA, USA) was used to generate ADV within the gels. Acoustic pulses generated by the transducer – 10 cycles, 10 ms pulse repetition period, 12.9 MPa peak compressional pressure (free field), 6.0 MPa peak rarefactional pressure (free field) – were achieved using a master function generator (33120A, Agilent Technologies, Palo Alto, CA, USA) gated by a secondary function generator (3314A, Agilent Technologies). The driving signal was sent to a power amplifier (60 dB, model 350, Matec Instrument Co., Northborough, MA, USA) and then directly to the transducer. The general approach to exposing the scaffolds to ultrasound was to fixture the plate in which the hydrogels were cast at the air–water interface of a 37 °C water bath. Acoustic pulses were transmitted through the bottom of the plate into each sample. The transducer was moved to expose the entirety of each gel to ultrasound until vaporization was complete, as assessed visually by cessation of bubble formation; the typical exposure time for complete vaporization was ~15 s. No temperature increases were observed in the gels using the aforementioned exposure setup and acoustic conditions. Sham controls were placed in the tank for a comparable time but not exposed to ultrasound. To demonstrate spatial patterning of ADV within the composites, the ultrasound transducer was rastered via a computer-controlled positioning system at a speed of 1 mm s^{-1} in a pre-defined pattern.

2.4. Composite morphology

Morphological features of droplet–hydrogel composites before and after ADV were characterized macroscopically by photography as well as microscopically using transmitted light and confocal fluorescence. Within 1 h of ultrasound or sham treatment, gels were rinsed briefly in PBS and mounted on microscope slides in coverwell imaging chambers with a small volume of PBS. Using an inverted SP5X microscope with a 10× objective, gross morphological features of the composites were captured by imaging transmitted light from the 488 nm line of an argon laser (Leica). Ultrastructural features of the fibrin scaffold were captured by imaging the fluorescence of AF647-tagged fibrinogen that was excited with the 647 nm line of a supercontinuum white light laser (Leica). Fluorescence images were captured at 5 μm intervals through 100 μm thick stacks. ImageJ (ver 1.47b, National Institutes of Health, USA) was used to uniformly adjust the brightness and contrast in images of transmitted light and to construct maximum projections of the stacks of fluorescence images.

2.5. Rheological testing

The mechanical properties of droplet–hydrogel composites were measured by dynamic torsion tests. Within ~6 h of sham or ultrasound exposures, samples were cut to 8 mm diameter with a biopsy punch (Miltex, York, PA, USA) and the thickness was measured in three locations using digital calipers (Mitutoyo, Kawasaki, Japan). Each sample was then loaded between platens in an AR-G2 rheometer (TA Instruments, New Castle, DE, USA). The test geometry consisted of an 8 mm diameter upper plate parallel with a temperature-regulated base plate set to 37 °C. Both surfaces were fit with adhesive-backed waterproof emery paper (3M, St Paul, MN, USA) to minimize slip. Samples were compressed by 10% of the initial thickness and allowed to equilibrate for 5 min. The samples were then subjected to oscillatory shear at 0.1 and 1 Hz with a strain amplitude of 1%. Measurements of the complex shear modulus (G^*) and dissipation factor (i.e., tangent of the phase angle, δ) reflect the stiffness and viscoelasticity of the materials, respectively.

2.6. In vitro release of bFGF

Gels were prepared as described above except that 0.1 U ml^{-1} aprotinin from bovine lung (Sigma–Aldrich) was included. After polymerization, each gel was covered with 1 ml endothelial basal medium (EBM, ENDO-Basal medium, Angio-Proteomie, Boston, MA, USA) supplemented with 10 μg ml^{-1} heparin (Sigma–Aldrich) and 5% fetal bovine serum (FBS, Hyclone, Thermo Scientific, Logan, UT, USA). Ultrasound and sham treatments were applied to the scaffolds as described above and then moved to a standard tissue culture incubator. Every 24 h for 6 days, 50% of the medium was collected and replaced with fresh medium. After 5 days, sham controls were exposed to ultrasound to evaluate the potential for delayed release of bFGF. The concentration of bFGF in the releasates was measured by ELISA.

To assess the bioactivity of bFGF released through ADV, a portion of each releasate was applied to monolayer cultures of human umbilical vein endothelial cells (HUVECs, Angio-Proteomie). The cells were initially plated at 1.25×10^4 cells cm^{-2} in a 96-well dish in endothelial growth medium (EGM, ENDO-Growth medium, Angio-Proteomie). After 24 h, the medium was replaced with EBM supplemented with 5% FBS and the next day the cells were treated with releasates from the droplet–hydrogel composites. Control cultures were treated with 0–5 ng ml^{-1} bFGF in EBM with 5% FBS and 10 μg ml^{-1} heparin. Every 24 h the medium was replaced with 100 μl of releasate collected that day (i.e. 10% of the total collected volume). After 5 days the metabolic activity of the cultures was assessed by the alamarBlue assay (Invitrogen) according to the manufacturer's instructions. Briefly, the cells were incubated with 10% (v/v) alamarBlue reagent in EBM for 2.5 h, and the fluorescence (λ_{ex}: 550 nm/λ_{em}: 590 nm) of the supernatants was measured in a Spectramax Gemini plate reader (Molecular Devices, Sunnyvale, CA, USA).

2.7. Viability of co-encapsulated cells and cell-mediated fibrinolysis

Droplet–hydrogel composites were prepared as described above except that either 1.25×10^5 HUVECs or cells of the mouse multipotent line C3H10T1/2, clone 8 (ATCC, catalog number CCL-226, Manassas, VA, USA) were co-encapsulated in each of the 0.5 ml gels along with 0%, 1% or 5% (v/v) double emulsion and 9.4 μg (5 mg ml^{-1} fibrin) or 18.8 μg (10 mg ml^{-1} fibrin) AF647-fibrinogen. These two cell populations were selected to assess any cell type-specific responses to ADV in the composites. In order to isolate the effects of ADV on cell viability, sham (i.e., without bFGF) emulsion was used for the composites. After polymerization, the gels were covered with 1 ml EGM for HUVECs or DMEM with penicillin/streptomycin and 10% FBS for C3H10T1/2 cells. A subset of the cell–gel constructs were then exposed to sham or ultrasound treatment as described above and placed in an incubator under standard cell culture conditions (37 °C, 5% CO_2, 95% relative

humidity). After 48 h, the conditioned medium was collected and portions were assayed for AF647 fluorescence (λ_{ex}: 620 nm /λ_{em}: 690 nm), using a Spectramax Gemini plate reader, as an indicator of cell-mediated fibrinolysis. Some constructs were incubated for 2.5 h in 10% (v/v) alamarBlue reagent, and the supernatants were assayed for fluorescence of the metabolized product as described above. Separate constructs were used for live/dead staining. The constructs were incubated for 1 h at 37 °C with 5 μM 5-chloromethylfluorescein diacetate ("Live" stain: CMFDA, Invitrogen) and 10 μg ml^{-1} propidium iodide ("Dead" stain: PI, Invitrogen) diluted in DMEM with 10% FBS. The constructs were washed twice with PBS for 15 min at 37 °C and then mounted on microscope slides in coverwell imaging chambers. Images of CMFDA- and PI-labeled cells and AF647-labeled fibrin were captured with an SP5X microscope and a 10× objective.

2.8. Fibrinolysis with plasmin

In order to assess the effects of droplets and ADV on enzymatic degradation of the fibrin hydrogel, we conducted experiments with cell-free constructs incubated with plasmin. Gels were prepared as described above except with 15 μg AF647-fibrinogen added to each 0.5 ml gel. After polymerization, gels were treated with sham or ultrasound exposures and then overlaid with DMEM supplemented with 2.5 μg ml^{-1} human plasmin (Sigma–Aldrich) and incubated at 37 °C. Aliquots of the DMEM were taken at various time points and analyzed for AF647 fluorescence, as described above.

2.9. Statistics

Data are expressed as the mean ± standard deviation of 3–5 samples per experimental group. ELISA and fluorescence assays were performed in duplicate or triplicate and averaged for each sample. Analysis of variance (ANOVA) was used to establish the significance between experimental groups. The Tukey–Kramer method, evaluated in MATLAB (The MathWorks Inc., Natick, MA, USA), was used to determine statistically significant differences between multiple groups, with differences deemed significant for $p < 0.05$.

3. Results

3.1. Characterization of emulsion

Fig. 1 displays a micrograph of the double emulsion structure used to encapsulate bFGF. For clarity, a relatively large droplet is shown, though smaller droplets exhibited similar double emulsion structures. The mean outer droplet diameter was 4.1 ± 0.3 μm with 0.7% (by number) and 87.3% (by volume) of the double emulsion droplets greater than 100 μm (Fig. 2). No differences in emulsion structure or particle size were observed when comparing sham emulsions vs. emulsions containing bFGF or fluorescein in the W_1 phase. Analysis of the supernatant indicated that >99% of bFGF remained encapsulated in the emulsion after washing.

3.2. Morphology of droplet–hydrogel composites

As seen macroscopically in Fig. 1 (inset), bubbles can be spatially patterned within the composite scaffold by rastering a focused ultrasound transducer (−6 dB lateral beam width: 0.8 mm). For a 10 mg ml^{-1} gel with 5% (v/v) emulsion, the lateral and axial dimensions of the bubble cloud (i.e. opaque features) were 0.8 mm and 3–4 mm, respectively. For a range of fibrin densities and emulsion volume fractions (Table 1), we used transmitted light and confocal fluorescence microscopy to characterize droplet- and ADV-induced changes in the ultrastructure of fibrin scaffolds (Fig. 3). Control gels lacking droplets exhibited a nearly homogeneous distribution of AF647-fibrinogen and few structures visible by transmitted light; we found no differences in scaffold morphology between ultrasound-exposed and

sham controls (not shown). Composite gels containing 1% or 5% emulsion exhibited numerous round opacities in the transmitted light images and gaps in the fluorescence, indicating that the fibrin polymerized around the droplets. Exposure of the composite gels to ultrasound induced vaporization of the emulsion and the generation of bubbles/pores ranging in size from tens of microns to millimeters in diameter. Fluorescence images revealed a consolidation of the fibrin at the margins of these bubbles, as indicated by an elevated fluorescence intensity in those regions. Qualitatively, droplets in the 5 mg ml^{-1} fibrin scaffolds yielded larger bubbles than in the 10 mg ml^{-1} scaffolds, and there were fewer unvaporized droplets following ultrasound exposure in the lower density fibrin. In contrast to the gels with 1% emulsion, gels with 5% emulsion appeared to establish an interconnected network of bubbles/pores. These results show that ADV can be used to introduce bubbles and thereby modify the ultrastructure of droplet–hydrogel composites.

3.3. Mechanical properties of droplet–hydrogel composites

Dynamic shear tests demonstrated that ADV caused dramatic increases in the stiffness of acoustic droplet–fibrin composites. The addition of emulsion without exposure to ultrasound did not change the shear properties of the composite for any of the formulations examined. But after exposure to ultrasound and vaporization of the emulsion, the droplet–hydrogel composite scaffolds exhibited substantial and statistically significant increases in the complex shear modulus, $|G^*|$, compared to sham-treated controls (Fig. 4A). In the lower density fibrin gels, vaporization of 1% emulsion increased the shear stiffness by ~300% and vaporization of 5% emulsion increased the shear stiffness by 1600–2100%. The higher density fibrin gels exhibited less robust increases in shear properties, with vaporization of 1% emulsion increasing stiffness by ~50% and vaporization of 5% emulsion increasing the stiffness by ~500% over sham controls. These increases were evident at both 0.1 and 1 Hz test frequencies. The increases in shear stiffness following ADV were also generally accompanied by increases in tan δ, which is an indicator of the viscoelasticity of the material. Higher values of tan δ indicate a more dissipative mechanical response. For 5 mg ml^{-1} fibrin with 1% emulsion and 10 mg ml^{-1} fibrin with either 1% or 5% emulsion, the ADV-induced increases in tan d were statistically significant (Fig. 4B). These results show that ADV can be used to modify the mechanical properties of droplet–hydrogel composites.

3.4. ADV-triggered release of bFGF from acoustic droplets

Fig. 5 shows that droplet–hydrogel composites exposed to ultrasound released significantly more bFGF than sham-treated controls, with peaks in release occurring between days 2 and 3. Low levels of release from sham controls were detected throughout the experiment and were independent of fibrin density. After exposure to ultrasound on the fifth day, the day 6 rates of release of sham controls with 5% emulsion were significantly greater than on day 5, indicating that a “delayed release” could be induced by delaying ADV. Ultrasound-treated 5 mg ml^{-1} fibrin gels with 5% emulsion released ~50 ng of bFGF over 6 days, or ~39% of the total bFGF initially loaded in each gel whereas ultrasound-treated 10 mg ml^{-1} fibrin gels with 5% emulsion released ~20% of the initial bFGF. For 5 mg ml^{-1} fibrin gels with 1% emulsion, ultrasound-treated samples released 2.5-fold more bFGF than sham controls over the first 5 days of the experiment. Five times more bFGF was released from ultrasound-treated samples than controls for 5 mg ml^{-1} fibrin gels with 5% emulsion. For both doses of emulsion in 10 mg ml^{-1} fibrin, the ultrasound-induced increases in bFGF were approximately 2-fold higher than the respective sham controls. These data demonstrate that droplet–hydrogel composites can provide controlled release of a growth factor in vitro.

The bioactivity of bFGF released by ADV in droplet–hydrogel composites was evaluated by culturing HUVECs with the releasates from the release study. This approach was based on the premise that bioactive bFGF would increase the metabolic activity of the cell cultures by

promoting survival and/or stimulating proliferation. After 5 days of treatment, we found that HUVECs treated with releasates from ultrasound-exposed droplet–hydrogel composites exhibited significantly higher metabolic activities than their respective sham controls for 5 mg ml^{-1} fibrin with 1% (92% increase) or 5% emulsion (48% increase) and 10 mg ml^{-1} fibrin with 1% (49% increase) or 5% droplets (39% increase) (Fig. 6). These results show that bFGF released by ADV is functional and bioactive.

3.5. Responses of cells to droplet–hydrogel composites

The viability of two cell types, primary HUVECs and the C3H10T1/2 mesenchymal progenitor line, cultured in sham- and ultrasound-treated droplet–hydrogel composites, was evaluated quantitatively by metabolic assay and qualitatively by live/dead staining and confocal fluorescence microscopy. After 48 h of in vitro culture, we detected few differences in the metabolic activity between groups. In HUVEC cultures, there were modest but statistically significant increases in the metabolic activity of 10 mg ml^{-1} fibrin gels with 0% or 1% droplets treated with ultrasound compared to sham controls (Fig. 7A). These differences were not detected in analogous C3H10T1/2 cultures (Fig. A1.A).

The release of AF647-fibrinogen from gels containing either HUVECs or C3H10T1/2 cells is displayed in Fig. 7B and Fig. A1.B, respectively. We detected several significant, but modest, differences in the release of AF647 between various groups. For 5 mg ml^{-1} fibrin gels containing HUVECs, ultrasound treatment caused a 7.9% and 12.5% decrease in released fibrinogen concentration for scaffolds with 1% and 5% emulsion, respectively. Similarly, ultrasound caused decreases of 11.1% and 14.7% for the 5 mg ml^{-1} gels containing HUVECs with 1% and 5% emulsion, respectively, compared to 0% emulsion sham controls. In gels containing C3H10T1/2 cells, the largest difference in fibrinogen release was a 7.9% decrease in 5 mg ml^{-1} fibrin with 5% emulsion and ultrasound treatment compared to sham controls with 0% emulsion. No differences were detected for either cell type in 10 mg ml^{-1} fibrin gels. Thus vaporization of droplets can in some cases slightly reduce cell-mediated release of fibrin in vitro.

Fig. A2 shows representative release profiles of AF647 fibrinogen from cell-free gels incubated with plasmin. No statistically significant differences ($p > 0.05$) were observed between gels without emulsion, with 1% or 5% emulsion and with 1% or 5% emulsion and ultrasound treatment (data for 1% emulsion not shown). These data indicate that neither the introduction of droplets nor the vaporization of droplets within the fibrin alters the susceptibility of the fibrin to degradation by exogenous proteases.

Confocal microscopy of live/dead-stained constructs confirmed the results of the metabolic assays. For HUVECs in 5 mg ml^{-1} fibrin composites, regardless of treatment group, 80–90% of cells were positive for CMFDA labeling (i.e. $CMFDA^+$) and negative for PI labeling (i.e. PI^-) after 48 h of culture (Fig. 7C). Although there appeared to be modest decreases in CMFDA labeling in ultrasound-treated constructs compared to sham controls, these differences did not reach statistical significance. Similar results were obtained with 10 mg ml^{-1} fibrin gels and C3H10T1/2 populated constructs (data not shown). Both $CMFDA^+$ and PI^+ cells were detected in close proximity to the margins of ADV-generated bubbles and pores. These results show that neither the droplet–hydrogel composites nor the ADV process generated statistically significant differences in cell viability.

4. Discussion

Sonosensitive emulsions and microbubbles have been studied extensively in the fields of diagnostic and therapeutic ultrasound, typically for contrast-enhanced imaging, intravascular delivery, and applications in cancer treatment [41,52,53]. The potential for these vehicles to

be applied in tissue regeneration is relatively unexplored. Microbubbles have been used as porogens [54,55] and carriers of growth factors [45] in the fabrication of scaffolds for tissue engineering, although the functions of microbubbles in these applications did not involve exposure to ultrasound. Liposome–microbubble–hydrogel composites treated with low frequency (20 kHz) ultrasound exhibited cavitation-based release of a model payload from the liposomes and afforded impressive control of release kinetics [56], but it is unclear how the cavitation required for release will affect the bioactivity of a therapeutic payload or the viability of invading cells. In addition, the use of low frequency ultrasound limits the spatial resolution of the release. Previously, we have shown that ultrasound in the range of 1–10 MHz can enhance the release of a protein-based therapeutic (thrombin) from a PFC double emulsion for intravascular delivery [32]. Similar PFC emulsions, without a therapeutic payload, are well-tolerated in the circulation of large animal models at doses up to ~10^8 droplets kg^{-1} [57]. Since ultrasound in the megahertz frequency range is used to trigger ADV, release of a therapeutic payload can be localized to a volume on the order of cubic millimeters. Here we describe novel composite materials that incorporate sonosensitive droplets, loaded with an angiogenic growth factor, in a biodegradable hydrogel scaffold. We demonstrate selective, ultrasound-induced release of the growth factor and alteration of scaffold properties.

Exposure of acoustic droplet–hydrogel composites to ultrasound readily induced the formation of bubbles in all of the formulations examined. Interestingly, bubble number and size appeared to be inversely related to fibrin density, suggesting that formation and growth of the bubbles can be reduced by increasing the stiffness of the surrounding hydrogel. This observation is consistent with the finding that the acoustic pressure threshold for vaporization of PFC emulsions increases with the viscosity of the surrounding medium [58]. The vaporization threshold is also dependent on droplet size, where large droplets are expected to vaporize more readily than small droplets. Indeed, for both densities of fibrin tested, we observed an unvaporized fraction of droplets following ultrasound exposure that was comprised primarily of smaller (<20 μm diameter) droplets, indicating that these droplets were exposed to acoustic pressures that were below their ADV thresholds. As expected, increasing the volume fraction of droplets in the composites increased the number of bubbles formed following exposure to ultrasound but did not appear to otherwise influence ADV. Although not observed in these studies, it is possible that at higher droplet concentrations acoustic “shadowing” will occur in which ADV-generated bubbles scatter incoming ultrasound energy and block the vaporization of droplets in the far field [59]. Quantitative studies of bubble formation and growth are required to verify the qualitative observations made here, but our findings are consistent with theory and previous experiments demonstrating that ADV thresholds can be “tuned” through modulation of droplet size and material properties of the surrounding medium.

ADV-generated PFC bubbles may provide a structural template for increasing the pore size of the fibrin scaffold. A wide range of pore sizes within a scaffold can be conducive for a variety of regenerative processes, such as fibroblast ingrowth (5–15 μm) or rapid vascularization (>500 μm) [60]. In the presented in vitro studies, most of the bubbles examined by transmitted and fluorescence microscopy remained filled with gas, although some bubbles (typically at the surfaces of the gels) were filled with fluid, indicating that the PFC gas had escaped. Many bubbles were clustered together and exhibited breaches in the fibrin scaffold between adjacent bubbles, indicating that formation of a semi-continuous pore network is possible with ADV. Although retention of PFC may be useful in some scenarios (e.g. delivery of dissolved oxygen within a thick construct [61]), gas-filled bubbles present barriers to cellular invasion and transport of nutrients. Clearance of PFC gas from the composite materials in vivo will depend on initial proximity to a vascular supply and subsequent invasion during angiogenesis. We speculate that gas exchange in the bubbles for

interstitial fluid will establish a fluid-filled pore network that is more amenable to solute transport and vascular invasion than pre-ADV composites or bubble-filled composites post-ADV. Future studies designed to assess the in vivo fate and local bioeffects of ADV-generated PFC gas are required to address this issue.

ADV increased the stiffness of acoustic droplet–hydrogel composites. The results of dynamic torsion tests showed that the complex shear modulus increased several fold, in an emulsion dose-dependent fashion, following exposure to ultrasound for the two densities of fibrin we examined. A previous study demonstrated that the inclusion of microbubbles within a hydrogel scaffold increased the elastic modulus [56]. The increases in stiffness after ADV may be attributed, in part, to the consolidated fibrin at the margins of the bubbles. During ADV, the PFC phase of the droplets undergoes a substantial volume expansion (~150-fold in water) [27] that in the composites is partially resisted and partially dissipated by the fibrin scaffold. The pressure in the bubble is sufficient to deform the fibrin such that the network is consolidated in the radial direction (with respect to the bubble) and stretched in the circumferential direction. Fibrin exhibits robust strain-stiffening behavior in which the storage modulus increases up to 40-fold over the range of 10–40% shear strain [62,63]. It is likely that the local increase in fibrin stiffness associated with the circumferential stretch imparted by the bubbles contributes to the increases in bulk modulus for ultrasound-treated composites. Ultrasound-treated droplet–hydrogel composites also exhibited, in general, higher dissipation factors (tan (δ)) than their respective sham-treated control gels. The sources of the more viscous mechanical responses are unclear but might include drag associated with the gas–liquid interface, bubble rearrangement or added molecular-level relaxations in the fibrin network due to the applied stretch. Collectively, these ADV-induced changes in hydrogel mechanical properties may have utility in directing the behavior of cells entrapped within, or migrating into, the composite materials. Previous studies have demonstrated that mesenchymal progenitors are sensitive to both the elastic modulus [18] and loss (viscous) modulus [64] of their substrate. In addition, spatially restricted changes in scaffold mechanics may be induced through targeted application of ultrasound for the generation of graded constructs such as osteochondral interfaces.

Ultrasound caused significant increases in the amount of bFGF released from the growth-factor-loaded composite scaffolds. A larger differential release (i.e. sham vs.+US) was observed from the 5 mg ml^{-1} gels than the 10 mg ml^{-1} gels, which is consistent with the observation that more unvaporized emulsion remained in the higher fibrin density gels after ultrasound exposure. For the release study, the ultrasound propagation path was through the bottom of a polystyrene well dish, which has an acoustic attenuation of ~4.5 dB cm^{-1} MHz^{-1} [65]. The use of a more acoustically transparent exposure window (ex. ~ 0.7 dB cm^{-1} MHz^{-1} for a silastic-bottomed BioFlex plate [65]) could minimize the amount of unvaporized emulsion. By comparison, we measured the attenuation coefficient of the 10 mg ml^{-1} fibrin scaffolds with 0% emulsion to be in the range of 0.04–0.14 dB cm^{-1} MHz^{-1}, which is lower than the attenuation of soft tissue (0.2–0.5 dB cm^{-1} MHz^{-1}) [66].

The release of bFGF in the absence of ultrasound is attributed to two potential mechanisms: (1) the diffusion of bFGF from the W_1 phase into the surrounding gel medium in the absence of droplet vaporization and (2) spontaneous vaporization of the PFC phase of the emulsion. Some spontaneous vaporization of the emulsion was observed in sham gels during the 6-day incubation period, suggesting that the boiling point elevation experienced by the PFP double emulsion is different from that experienced by single PFP emulsions [36,37]. Spontaneous vaporization could be minimized by using a PFC with a higher boiling point or by minimizing the fraction of large PFP droplets, which are more likely to spontaneously vaporize [37]. Increasing the density/stiffness of the hydrogel may also establish less permissive conditions for spontaneous vaporization. Despite low levels of spontaneous

vaporization, exposure of the sham controls to ultrasound at day 5 caused a statistically significant increase in the amount of bFGF released on day 6. Thus, acoustic droplet–hydrogel composites can function as “on-demand” growth factor delivery vehicles, with focused or unfocused ultrasound serving as the non-invasive stimulus for release.

Release of bFGF from 10 mg ml^{-1} fibrin composites was slower and cumulatively lower than that from 5 mg ml^{-1} gels. As described above, this may be attributed in part to a higher ADV threshold in the denser gels, which would reduce the number of vaporizable droplets and bFGF available for release upon exposure to a given ultrasound stimulus. Fibrin scaffolds exhibit density-dependent transport properties as well, as evidenced by a two-to three-fold reduction in effective diffusion coefficient for an increase in fibrin density from 2.5 mg ml^{-1} to 10 mg ml^{-1} [67]. Fibrin can also bind bFGF [68], however, and since the number of binding sites increases with fibrin density, such diffusion-limiting interactions are expected to have a greater effect in the 10 mg ml^{-1} fibrin gels than in the lower density fibrin. In the context of therapeutic angiogenesis, retention of ADV-released bFGF within the hydrogel may be useful for establishing chemotactic gradients, and bFGF-fibrin complexes provide a higher proliferative stimulus to endothelial cells than bFGF alone [69]. Alternatively, hydrogel scaffolds with lower protein affinities (e.g. polyethylene glycol) and/or more open pore structures may be used in place of fibrin to permit complete release of the payload carried by the acoustic droplets.

Under certain acoustic conditions, ultrasound has been shown to alter the structure and function of solubilized proteins [70,71]. Fig. 6 demonstrates that bFGF released by ADV is functionally bioactive. Computing the bioactivity of released bFGF relative to the amount of bFGF initially loaded into the emulsion is not straight-forward with this dataset. However, based on the metabolic activities of cell cultures treated with known concentrations of bFGF and the measured concentrations of bFGF in the releasates, we estimate relative bioactivities of 13–48%, thus indicating that some bioactivity of the growth factor is lost upon either emulsion preparation and/or vaporization. If the reduction in bioactivity is due to effects caused by inertial cavitation, which is the rapid growth and violent collapse of a gas bubble, then ADV could be generated with a higher frequency transducer [72] or shorter pulses [73]. Since the acoustic threshold for ADV is inversely related to frequency [74], the use of a higher frequency transducer would permit the use of lower pressures while also having increased spatial resolution, though at the cost of penetration depth.

A previous study demonstrated that ADV occurring adjacent to adherent cells, within culture medium, caused cell detachment and potentially cell death [31]. This is likely due to the elevated fluid velocities and shear forces generated during the conversion of the liquid PFC droplets into microbubbles [39]. In contrast, ADV of emulsion contained with the droplet–hydrogel composite did not affect viability of two different cell types and only caused slight reductions in cell-mediated release of AF647-labeled fibrin in vitro at a density of 5 mg ml^{-1}. Thus, it appears that fibrin gels inhibit cytotoxic effects stemming from ADV, with the inhibition related to gel density. The mechanisms by which the hydrogel component of the composites limits ADV-induced cytotoxicity were outside the scope of the current study, but warrant further investigation, including determining the occurrence of inertial cavitation. For some conditions, ultrasound stimulated the metabolic activity of HUVECs within the scaffolds, which is consistent with previous findings [75,76]. These results suggest that the acoustic droplet–hydrogel composites are also suitable carriers for populations of cells that can participate in regenerative processes such as angiogenesis. Future studies will examine the potential for ADV to regulate phenotypic changes (e.g. differentiation) in cells suspended in these composites and in adjacent tissue.

5. Conclusions

The results of this study demonstrate the potential for acoustic droplet–hydrogel composites to function as drug delivery vehicles as well as modifiers of scaffold architecture and mechanical properties. Through the application of focused ultrasound, release of growth factors or other regenerative factors from these materials may be triggered “on-demand” in non-invasive and spatially and temporally restricted manners. ADV-released growth factor was bioactive, and the viability of cells encapsulated within the composites was not affected by ADV. Collectively, our results suggest that this novel platform will have tremendous utility in tissue engineering and regeneration. The formulations presented in these studies are amenable to injection at sites of injury, and future studies are aimed at characterizing the in vivo performance of these materials.

Supplementary Material

Refer to Web version on PubMed Central for supplementary material.

Acknowledgments

We thank Dr Andrew Putnam for use of the rheometer, Rahul Singh for technical support of the rheological tests, and Dr Oliver Kripfgans for helpful discussions. This work was supported through NIH grant R01DE013386-09 (RTF) and Department of Defense grant OR090134 (RTF & JBF). CGW was supported by a postdoctoral training fellowship administered by NIDCR (T32DE007057-34).

References

[1]. Shaikh FM, Callanan A, Kavanagh EG, Burke PE, Grace PA, McGloughlin TM. Fibrin: a natural biodegradable scaffold in vascular tissue engineering. Cells Tissues Organs. 2008; 188:333–46. [PubMed: 18552484]

[2]. Dehghani F, Annabi N. Engineering porous scaffolds using gas-based techniques. Curr Opin Biotechnol. 2011; 22:661–6. [PubMed: 21546240]

[3]. Seliktar D. Designing cell-compatible hydrogels for biomedical applications. Science. 2012; 336:1124–8. [PubMed: 22654050]

[4]. Kuhl PR, GriffithCima LG. Tethered epidermal growth factor as a paradigm for growth factor-induced stimulation from the solid phase. Nat Med. 1996; 2:1022–7. [PubMed: 8782461]

[5]. Li B, Davidson JM, Guelcher SA. The effect of the local delivery of platelet-derived growth factor from reactive two-component polyurethane scaffolds on the healing in rat skin excisional wounds. Biomaterials. 2009; 30:3486–94. [PubMed: 19328544]

[6]. d’Angelo I, Garcia-Fuentes M, Parajo Y, Welle A, Vantus T, Horvath A, et al. Nanoparticles based on PLGA:poloxamer blends for the delivery of proangiogenic growth factors. Mol Pharm. 2010; 7:1724–33. [PubMed: 20681555]

[7]. Go DP, Gras SL, Mitra D, Nguyen TH, Stevens GW, Cooper-White JJ, et al. Multilayered microspheres for the controlled release of growth factors in tissue engineering. Biomacromolecules. 2011; 12:1494–503. [PubMed: 21413682]

[8]. Johnson MR, Lee HJ, Bellamkonda RV, Guldberg RE. Sustained release of BMP-2 in a lipid-based microtube vehicle. Acta Biomater. 2009; 5:23–8. [PubMed: 18838348]

[9]. Sojo K, Sawaki Y, Hattori H, Mizutani H, Ueda M. Immunohistochemical study of vascular endothelial growth factor (VEGF) and bone morphogenetic protein-2,-4 (BMP-2,-4) on lengthened rat femurs. J Craniomaxillofac Surg. 2005; 33:238–45. [PubMed: 15979317]

[10]. Bos PK, van Osch GJVM, Frenz DA, Verhaar JAN, Verwoerd-Verhoef HL. Growth factor expression in cartilage wound healing: temporal and spatial immunolocalization in a rabbit auricular cartilage wound model. Osteoarthritis Cartilage. 2001; 9:382–9. [PubMed: 11399103]

[11]. Matsusaki M, Akashi M. Novel functional biodegradable polymer IV: pH-sensitive controlled release of fibroblast growth factor-2 from a poly(gamma-glutamic acid)-sulfonate matrix for tissue engineering. Biomacromolecules. 2005; 6:3351–6. [PubMed: 16283765]

[12]. Thornton PD, McConnell G, Ulijn RV. Enzyme responsive polymer hydrogel beads. Chem Commun. 2005:5913–5.

[13]. Frimpong RA, Fraser S, Hilt JZ. Synthesis and temperature response analysis of magnetic-hydrogel nanocomposites. J Biomed Mater Res A. 2007; 80A:1–6. [PubMed: 16941587]

[14]. Zhao X, Kim J, Cezar CA, Huebsch N, Lee K, Bouhadir K, et al. Active scaffolds for on-demand drug and cell delivery. Proc Natl Acad Sci U S A. 2011; 108:67–72. [PubMed: 21149682]

[15]. Kulkarni R, Biswanath S. Electrically responsive smart hydrogels in drug delivery: a review. J Appl Biomater Biomech. 2007; 5:125–39. [PubMed: 20799182]

[16]. Wu C, Chen C, Lai J, Mu X, Zheng J, Zhao Y. Molecule-scale controlled-release system based on light-responsive silica nanoparticles. Chem Commun. 2008; 23:2662–4.

[17]. Lavigne MD, Pennadam SS, Ellis J, Yates LL, Alexander C, Gorecki DC. Enhanced gene expression through temperature profile-induced variations in molecular architecture of thermoresponsive polymer vectors. J Gene Med. 2007; 9:44–54. [PubMed: 17167816]

[18]. Engler AJ, Sen S, Sweeney HL, Discher DE. Matrix elasticity directs stem cell lineage specification. Cell. 2006; 126:677–89. [PubMed: 16923388]

[19]. Datta N, Pham QP, Sharma U, Sikavitsas VI, Jansen JA, Mikos AG. In vitro generated extracellular matrix and fluid shear stress synergistically enhance 3D osteoblastic differentiation. Proc Natl Acad Sci U S A. 2006; 103:2488–93. [PubMed: 16477044]

[20]. Boontheekul T, Hill EE, Kong HJ, Mooney DJ. Regulating myoblast phenotype through controlled gel stiffness and degradation. Tissue Eng. 2007; 13:1431–42. [PubMed: 17561804]

[21]. Marklein RA, Burdick JA. Spatially controlled hydrogel mechanics to modulate stem cell interactions. Soft Matter. 2010; 6:136–43.

[22]. Ramanan VV, Katz JS, Guvendiren M, Cohen ER, Marklein RA, Burdick JA. Photocleavable side groups to spatially alter hydrogel properties and cellular interactions. J Mater Chem. 2010; 20:8920–6.

[23]. Khanna A, Nelmes RTC, Gougoulias N, Maffulli N, Gray J. The effects of LIPUS on soft-tissue healing: a review of literature. Br Med Bull. 2009; 89:169–82. [PubMed: 19011263]

[24]. Iwashina T, Mochida J, Miyazaki T, Watanabe T, Iwabuchi S, Ando K, et al. Low-intensity pulsed ultrasound stimulates cell proliferation and proteoglycan production in rabbit intervertebral disc cells cultured in alginate. Biomaterials. 2006; 27:354–61. [PubMed: 16099036]

[25]. Claes L, Willie B. The enhancement of bone regeneration by ultrasound. Prog Biophys Mol Bio. 2007; 93:384–98. [PubMed: 16934857]

[26]. Apfel, RE. Activatable infusable dispersions containing drops of a superheated liquid for methods of therapy and diagnosis. Apfel Enterprises, Inc.; United States: 1998.

[27]. Kripfgans OD, Fowlkes JB, Miller DL, Eldevik OP, Carson PL. Acoustic droplet vaporization for therapeutic and diagnostic applications. Ultrasound Med Biol. 2000; 26:1177–89. [PubMed: 11053753]

[28]. Hwang TL, Lin YJ, Chi CH, Huang TH, Fang JY. Development and evaluation of perfluorocarbon nanobubbles for apomorphine delivery. J Pharm Sci. 2009; 98:3735–47. [PubMed: 19156914]

[29]. Rapoport N, Gao Z, Kennedy A. Multifunctional nanoparticles for combining ultrasonic tumor imaging and targeted chemotherapy. J Natl Cancer Inst. 2007; 99:1095–106. [PubMed: 17623798]

[30]. Fang JY, Hung CF, Hua SC, Hwang TL. Acoustically active pefluorocarbon nanoemulsions as drug delivery carriers for camptothecin: drug release and cytoxicity against cancer cells. Ultrasonics. 2009; 49:39–46. [PubMed: 18554679]

[31]. Fabiilli ML, Haworth KJ, Sebastian IE, Kripfgans OD, Carson PL, Fowlkes JB. Delivery of chlorambucil using an acoustically-triggered perfluoropentane emulsion. Ultrasound Med Biol. 2010; 36:1364–75. [PubMed: 20691925]

[32]. Fabiilli ML, Lee JA, Kripfgans OD, Carson PL, Fowlkes JB. Delivery of water-soluble drugs using acoustically triggered perfluorocarbon double emulsions. Pharm Res. 2010; 27:2753–65. [PubMed: 20872050]

[33]. Wang CH, Kang ST, Lee YH, Luo YL, Huang YF, Yeh CK. Aptamer-conjugated and drug-loaded acoustic droplets for ultrasound theranosis. Biomaterials. 2012; 33:1939–47. [PubMed: 22142768]

[34]. Couture O, Urban A, Bretagne A, Martinez L, Tanter M, Tabeling P. In vivo targeted delivery of large payloads with an ultrasound clinical scanner. Med Phys. 2012; 39:5229–37. [PubMed: 22894447]

[35]. Kagan D, Benchimol MJ, Claussen JC, Chuluun-Erdene E, Esener S, Wang J. Acoustic droplet vaporization and propulsion of perfluorocarbon-loaded microbullets for targeted tissue penetration and deformation. Angew Chem Int Ed Engl. 2012; 51:7519–22. [PubMed: 22692791]

[36]. Rapoport NY, Kennedy AM, Shea JE, Scaife CL, Nam K-H. Controlled and targeted tumor chemotherapy by ultrasound-activated nanoemulsions/microbubbles. J Control Release. 2009; 138:268–76. [PubMed: 19477208]

[37]. Sheeran PS, Wong VP, Luois S, McFarland RJ, Ross WD, Feingold S, et al. Decafluorobutane as a phase-change contrast agent for low-energy extravascular ultrasonic imaging. Ultrasound Med Biol. 2011; 37:1518–30. [PubMed: 21775049]

[38]. Wong ZZ, Kripfgans OD, Qamar A, Fowlkes JB, Bull JL. Bubble evolution in acoustic droplet vaporization at physiological temperature via ultra-high speed imaging. Soft Matter. 2011; 7:4009–16.

[39]. Kripfgans OD, Fabiilli ML, Carson PL, Fowlkes JB. On the acoustic vaporization of micrometer-sized droplets. J Acoust Soc Am. 2004; 116:272–81. [PubMed: 15295987]

[40]. Johnson JLH, Dolezal MC, Kerschen A, Matsunaga TO, Unger EC. In vitro comparison of dodecafluoropentane (DDFP), perfluorodecalin (PFD), and perfluoroctylbromide (PFOB) in the facilitation of oxygen exchange. Artif cells, Blood Substit Biotechnol. 2009; 37:156–62.

[41]. Diaz-Lopez R, Tsapis N, Fattal E. Liquid perfluorocarbons as contrast agents for ultrasonography and 19F-MRI. Pharm Res. 2010; 27:1–16. [PubMed: 19902338]

[42]. Riess JG. Oxygen carriers ("blood substitutes") - raison d'etre, chemistry, and some physiology. Chem Rev. 2001; 101:2797–919. [PubMed: 11749396]

[43]. Courrier HM, Vandamme TF, Krafft MP. Reverse water-in-fluorocarbon emulsions and microemulsions obtained with a fluorinated surfactant. Colloids Surf A. 2004; 244:141–8.

[44]. Rajian JR, Fabiilli ML, Fowlkes JB, Carson PL, Wang X. Drug delivery monitoring by photoacoustic tomography with an ICG encapsulated double emulsion. Opt Expr. 2011; 19:14335–47.

[45]. Couture O, Faivre M, Pannacci N, Babataheri A, Servois V, Tabeling P, et al. Ultrasound internal tattooing. Med Phys. 2011; 38:1116–23. [PubMed: 21452748]

[46]. Demirdogen B, Elcin AE, Elcin YM. Neovascularization by bFGF releasing hyaluronic acid-gelatin microspheres: in vitro and in vivo studies. Growth Factors. 2010; 28:426–36. [PubMed: 20854186]

[47]. Perets A, Baruch Y, Weisbuch F, Shoshany G, Neufeld G, Cohen S. Enhancing the vascularization of three-dimensional porous alginate scaffolds by incorporating controlled release basic fibroblast growth factor microspheres. J Biomed Mater Res A. 2003; 65A:489–97. [PubMed: 12761840]

[48]. Gomez G, Korkiakoski S, Gonzalez MM, Lansmann S, Ella V, Salo T, et al. Effect of FGF and polylactide scaffolds on calvarial bone healing with growth factor on biodegradable polymer scaffolds. J Craniofac Surg. 2006; 17:935–42. [PubMed: 17003623]

[49]. Behr B, Sorkin M, Lehnhardt M, Renda A, Longaker MT, Quarto N. A Comparative analysis of the osteogenic effects of BMP-2, FGF-2, and VEGFA in a calvarial defect model. Tissue Eng. 2012; 18:1079–86.

[50]. Clausell-Tormos J, Lieber D, Baret J-C, El-Harrak A, Miller OJ, Frenz L, et al. Droplet-based microfluidic platforms for the encapsulation and screening of mammalian cells and multicellular organisms. Chem Biol. 2008; 15:427–37. [PubMed: 18482695]

[51]. Sommer A, Rifkin DB. Interaction of heparin with human basic fibroblast growth-factor – protection of the angiogenic protein from proteolytic degradation by a glycosaminoglycan. J Cell Physiol. 1989; 138:215–20. [PubMed: 2910884]

[52]. Tinkov S, Bekeredjian R, Winter G, Coester C. Microbubbles as ultrasound triggered drug carriers. J Pharm Sci. 2009; 98:1935–61. [PubMed: 18979536]

[53]. Ibsen S, Benchimol M, Simberg D, Schutt C, Steiner J, Esener S. A novel nested liposome drug delivery vehicle capable of ultrasound triggered release of its payload. J Control Release. 2011; 155:358–66. [PubMed: 21745505]

[54]. Nair A, Thevenot P, Dey J, Shen JH, Sun MW, Yang J, et al. Novel polymeric scaffolds using protein microbubbles as porogen and growth factor carriers. Tissue Eng. 2010; 16:23–32.

[55]. Lima EG, Durney KM, Sirsi SR, Nover AB, Ateshian GA, Borden MA, et al. Microbubbles as biocompatible porogens for hydrogel scaffolds. Acta Biomater. 2012; 8:4334–41. [PubMed: 22868194]

[56]. Epstein-Barash H, Orbey G, Polat BE, Ewoldt RH, Feshitan J, Langer R, et al. A microcomposite hydrogel for repeated on-demand ultrasound-triggered drug delivery. Biomaterials. 2010; 31:5208–17. [PubMed: 20347484]

[57]. Zhang M, Fabiilli ML, Haworth KJ, Fowlkes JB, Kripfgans OD, Roberts WW, et al. Initial investigation of acoustic droplet vaporization for occlusion in canine kidney. Ultrasound Med Biol. 2010; 36:1691–703. [PubMed: 20800939]

[58]. Fabiilli ML, Haworth KJ, Fakhri NH, Kripfgans OD, Carson PL, Fowlkes JB. The role of inertial cavitation in acoustic droplet vaporization. IEEE Trans Ultrason Ferroelectr Freq Control. 2009; 56:1006–17. [PubMed: 19473917]

[59]. Lo AH, Kripfgans OD, Carson PL, Fowlkes JB. Spatial control of gas bubbles and their effects on acoustic fields. Ultrasound Med Biol. 2006; 32:95–106. [PubMed: 16364801]

[60]. Whang K, Healy KE, Elenz DR, Nam EK, Tsai DC, Thomas CH, et al. Engineering bone regeneration with bioabsorbable scaffolds with novel microarchitecture. Tissue Eng. 1999; 5:35–51. [PubMed: 10207188]

[61]. Maillard E, Juszczak MT, Clark A, Hughes SJ, Gray DRW, Johnson PRV. Perfluorodecalin-enriched fibrin matrix for human islet culture. Biomaterials. 2011; 32:9282–9. [PubMed: 21899883]

[62]. Bale MD, Ferry JD. Strain enhancement of elastic-modulus in fine fibrin clots. Thromb Res. 1988; 52:565–72. [PubMed: 3232126]

[63]. Shah JV, Janmey PA. Strain hardening of fibrin gels and plasma clots. Rheol Acta. 1997; 36:262–8.

[64]. Cameron AR, Frith JE, Cooper-White JJ. The influence of substrate creep on mesenchymal stem cell behaviour and phenotype. Biomaterials. 2011; 32:5979–93. [PubMed: 21621838]

[65]. Garvin KA, Hocking DC, Dalecki D. Controlling the spatial organization of cells and extracellular matrix proteins in engineered tissues using ultrasound standing wave fields. Ultrasound Med Biol. 2010; 36:1919–32. [PubMed: 20870341]

[66]. Wells PNT, Liang HD. Medical ultrasound: imaging of soft tissue strain and elasticity. J R Soc Interface. 2011; 8:1521–49. [PubMed: 21680780]

[67]. Ghajar CM, Chen X, Harris JW, Suresh V, Hughes CCW, Jeon NL, et al. The effect of matrix density on the regulation of 3-D capillary morphogenesis. Biophys J. 2008; 94:1930–41. [PubMed: 17993494]

[68]. Sahni A, Odrljin T, Francis CW. Binding of basic fibroblast growth factor to fibrinogen and fibrin. J Biol Chem. 1998; 273:7554–9. [PubMed: 9516457]

[69]. Sahni A, Khorana AA, Baggs RB, Peng H, Francis CW. FGF-2 binding to fibrin(ogen) is required for augmented angiogenesis. Blood. 2006; 107:126–31. [PubMed: 16160009]

[70]. Tian ZM, Wan MX, Wang SP, Kang JQ. Effects of ultrasound and additives on the function and structure of trypsin. Ultrason Sonochem. 2004; 11:399–404. [PubMed: 15302026]

[71]. Marchioni C, Riccardi E, Spinelli S, Dell'Unto F, Grimaldi P, Bedini A, et al. Structural changes induced in proteins by therapeutic ultrasounds. Ultrasonics. 2009; 49:569–76. [PubMed: 19278707]

[72]. Apfel RE, Holland CK. Gauging the likelihood of cavitation from short-pulse, low-duty cycle diagnostic ultrasound. Ultrasound Med Biol. 1991; 17:179–85. [PubMed: 2053214]

[73]. Atchley AA, Frizzell LA, Apfel RE, Holland CK, Madanshetty S, Roy RA. Thresholds for cavitation produced in water by pulsed ultrasound. Ultrasonics. 1988; 26:280–5. [PubMed: 3407017]

[74]. Kripfgans OD, Fowlkes JB, Woydt M, Eldevik OP, Carson PL. In vivo droplet vaporization for occlusion therapy and phase aberration correction. IEEE Transactions on Ultrasonics, Ferroelectrics, and Frequency Control. 2002; 49:726–38.

[75]. Doan N, Reher P, Meghji S, Harris M. In vitro effects of therapeutic ultrasound on cell proliferation, protein synthesis, and cytokine production by human fibroblasts, osteoblasts, and monocytes. J Oral Maxillofac Surg. 1999; 57:409–19. [PubMed: 10199493]

[76]. Altland OD, Dalecki D, Suchkova VN, Francis CW. Low-intensity ultrasound increases endothelial cell nitric oxide synthase activity and nitric oxide synthesis. J Thromb Haemost. 2004; 2:637–43. [PubMed: 15102020]

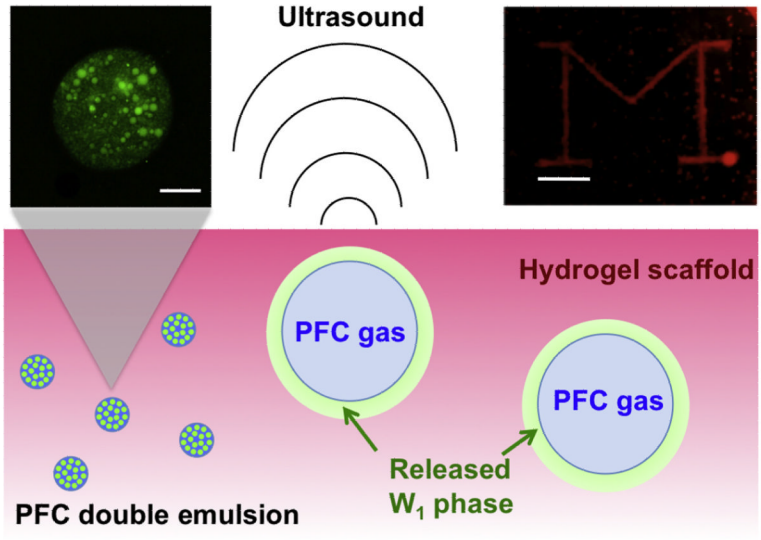

Fig. 1.

Schematic representation of drug release by ADV in a hydrogel scaffold. Bottom: A water-in-PFC-in-water (W_1/PFC/W_2) double emulsion, containing a growth factor in the W_1 phase, is encapsulated within the scaffold. Upon exposure to acoustic amplitudes greater than the ADV threshold of the emulsion, the PFC within the droplets is vaporized, thus releasing the W_1 phase. Top left: confocal fluorescence image (fluorescein, shown in green) of a PFC double emulsion droplet (scale bar = 10 μm). Smaller aqueous droplets, containing a water-soluble payload such as fluorescein or bFGF, are enveloped by a larger PFC globule. Top right: visible image of a 10 mg ml^{-1} fibrin gel containing 5% (v/v) double emulsion after targeted exposure to ultrasound. The “block M” consists of gas bubbles generated by ADV. Scale bar = 4 mm.

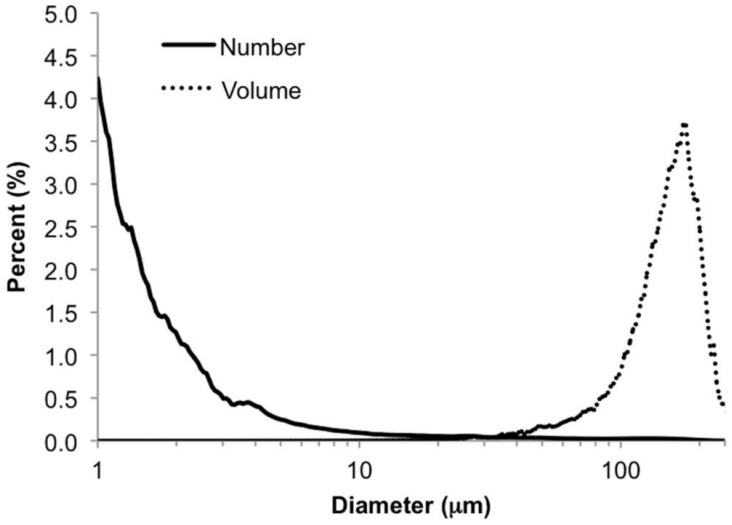

Fig. 2.
Number and volume-weighted size distributions of a PFC double emulsion containing bFGF. Droplets were sized using a Coulter counter within 2 h of preparation.

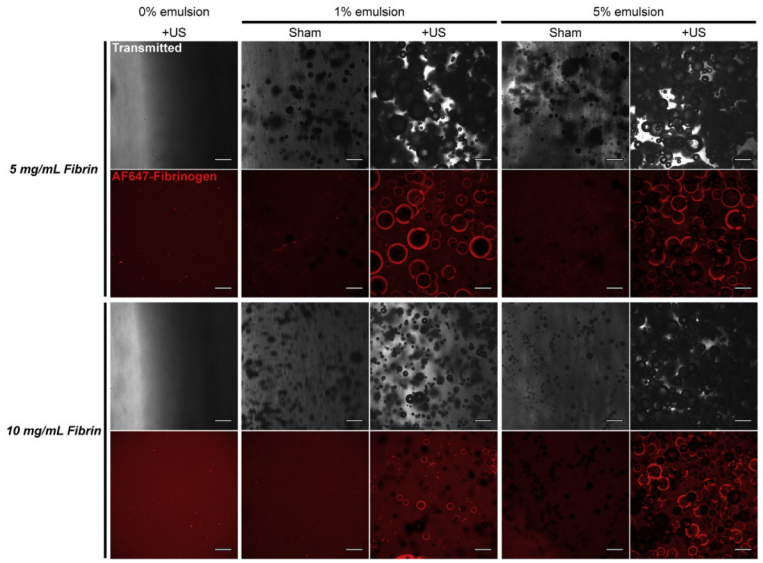

Fig. 3.

Morphologies of droplet–hydrogel composites with and without exposure to ultrasound (US). Representative images of transmitted light (488 nm, shown in grayscale) and maximum projections from 100 μm stacks of confocal fluorescence images (AF647-fibrinogen, shown in red) depict ADV-induced changes in scaffold architecture for 5 mg ml^{-1} and 10 mg ml^{-1} fibrin hydrogels doped with 0%, 1% or 5% (v/v) double emulsion. Panels at left show the morphology of fibrin hydrogels without droplets that were exposed to ultrasound; sham controls appeared similar. Due to the curved surfaces of the samples, we observed gradients in the intensity of transmitted light for the hydrogels without emulsion. Scale bars = 200 μm.

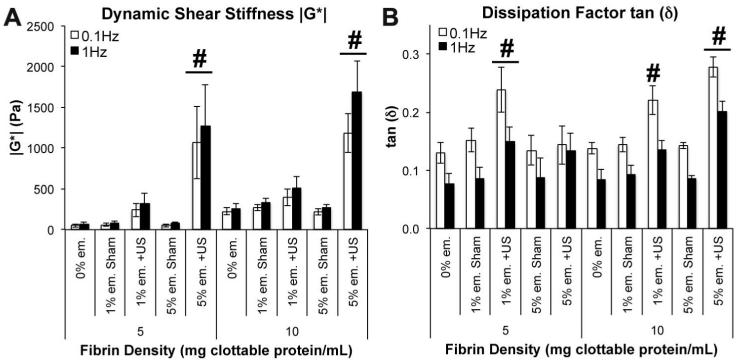

Fig. 4.

Mechanical properties of droplet–hydrogel composites with and without exposure to ultrasound (US). Oscillatory torsional shear tests (1% strain magnitude at 0.1 and 1.0 Hz) were used to measure the complex shear modulus $|G^*|$ (A) and dissipation factor tan (δ) (B) of the materials within ~6 h of sham or US treatment. Data are shown as mean± (B) of the materials win = 5. $^{\#}p < 0.05$ vs. sham controls.

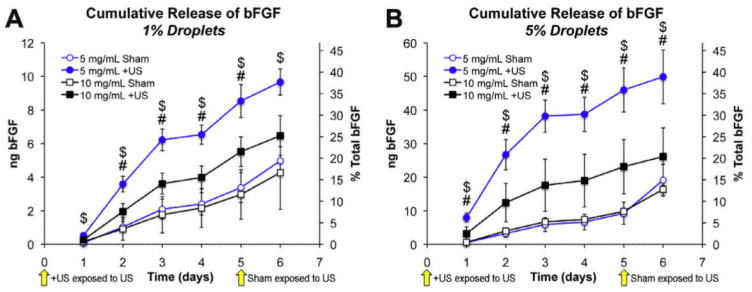

Fig. 5.

ADV-induced release of bFGF from droplet–hydrogel composites.+US groups were exposed to ultrasound at the start of the experiment (i.e. time = 0 days) and shams were exposed to ultrasound after collection of releasate on day 5. Cumulative release profiles are shown in (A) and (B). Blue series indicate 5 mg ml^{-1} fibrin and black series indicate 10 mg ml^{-1} fibrin. Data are shown as mean ± standard deviation for $n = 5$. $^{\$}p < 0.05$ for 5 mg ml^{-1} fibrin + US vs. sham control. $^{\#}p < 0.05$ for 10 mg ml^{-1} fibrin + US vs. sham control. For sham controls with 5% emulsion (for both 5 mg ml^{-1} and 10 mg ml^{-1} fibrin) treated with ultrasound at day 5, rates of release were found to be significantly higher at day 6 compared to projected values computed using the 95% confidence interval of the slope between days 1–5.

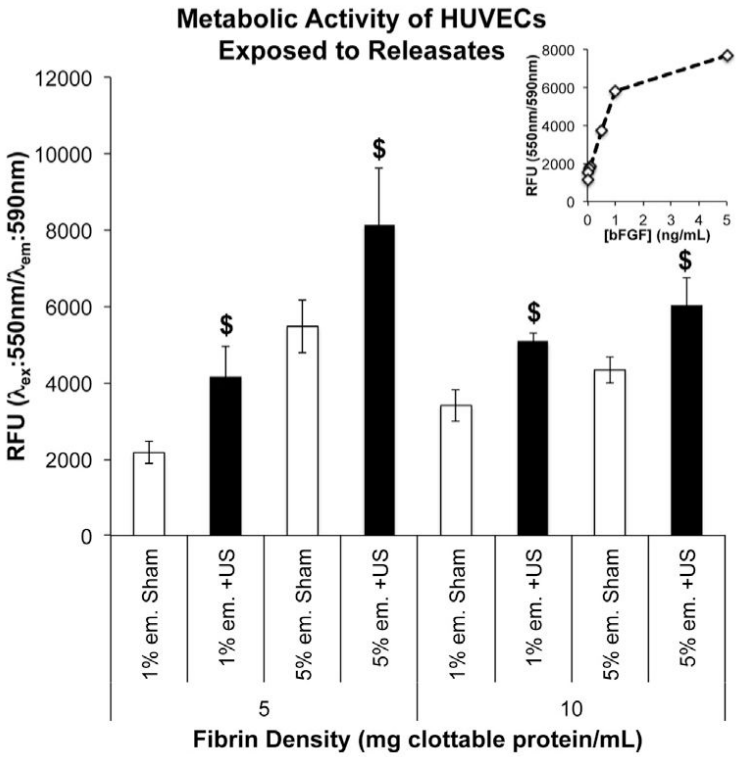

Fig. 6.

Metabolic activity of HUVECs after 5 days of incubation with releasates from droplet–hydrogel composites. Cells were incubated with releasates collected that day. Data are shown as mean ± standard deviation for $n = 5$. $^{\$}p < 0.05$ vs. sham control. Inset shows activity of HUVECs treated with known concentrations of bFGF.

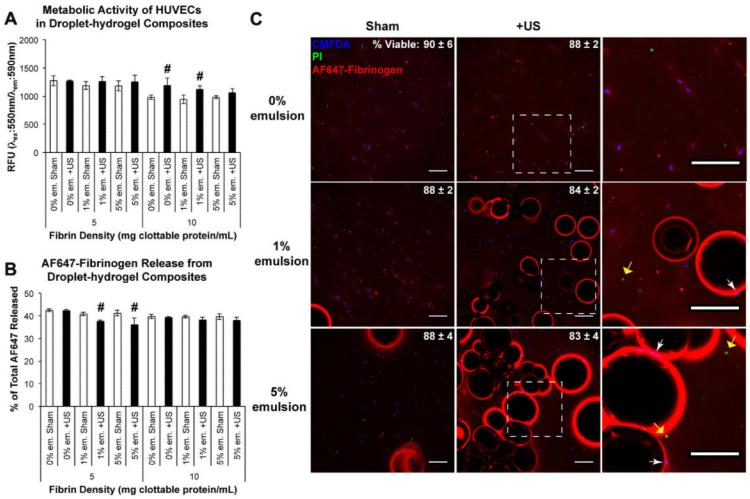

Fig. 7.

Effects of ultrasound (US) exposure on HUVECs in droplet–hydrogel composites. The metabolic activity (A) and release of AF647 fibrinogen (B) from HUVEC composites were measured 2 days after ADV. Data are shown as mean ± standard deviation for $n = 5$ (metabolic activity) and $n = 4$ (release). $^{\#}p < 0.05$ vs. sham control. CMFDA (blue)/PI (green) labeling of HUVECs in 5 mg ml^{-1} fibrin constructs demonstrates proximity of viable cells to bubbles formed by ADV (C). The percentage of viable cells (mean ± standard deviation; $n = 3$) for each condition is given in the upper right. The right column displays zoomed-in panels from the center column (denoted by the boxed regions). Viable (white arrows) and necrotic cells (yellow arrows) are observed adjacent to the bubbles. Scale bars = 200 μm.

Table 1

Composition of droplet–hydrogel scaffolds.

Composite formulation			
Fibrin (mg ml^{-1})	**Emulsion (% v/v)**	**bFGF (ng ml^{-1})**	**PFP (mg ml^{-1})**
5	0	0	0
5	1	51.3	3.3
5	5	256.4	16.7
10	0	0	0
10	1	51.3	3.3
10	5	256.4	16.7

The concentrations of bFGF and PFP are expressed per gel volume. The thrombin concentration was similar for all formulations (2 U ml^{-1}).